An overbounding ellipse approach for set based tracking with range-bearing measurements

Fiona Fletcher **M. Sanjeev Arulampalam**
Maritime Operations Division, Defence Science and Technology Organisation
PO Box 1500, Edinburgh, SA 5111
AUSTRALIA
Fiona.Fletcher@defence.gov.au Sanjeev.Arulampalam@defence.gov.au

Abstract – *In many tracking applications, the target state is estimated using range-bearing measurements. For statistical trackers, this problem may be dealt with using a converted measurement Kalman Filter. In this paper, measurement conversion procedures are proposed for using range-bearing measurements in a set based tracker. These procedures involve overbounding the range-bearing error region with an ellipse. The measurement conversions have been implemented in a set based tracker and numerical results are presented demonstrating their relative performance.*

Keywords: Set based estimation, tracking, range-bearing measurements

1 Introduction

It is common in target tracking applications for measurements from a target to be non-linearly related to the target state. A particularly prevalent example of this is where range-bearing measurements are obtained from a target whose state is modelled in Cartesian coordinates. This is often the case for active sonar or radar [1].

There are two main approaches for dealing with range-bearing measurements in statistical tracking. An Extended Kalman Filter (EKF) may be used, where the non-linear measurement equation is approximated by a linear equation using Taylor series expansion [2]. An alternative approach is that of the Converted Measurement Kalman Filter (CMKF), where the measurements are converted to Cartesian position and covariance and are then used in a linear Kalman Filter. Examples of these measurement conversions are the standard measurement conversion [2], the debiased measurement conversion [3] and the unbiased measurement conversion [4]. These trackers are all based around the Kalman filter, which calculates a Gaussian density for the target state based on assumptions of Gaussianity for the noises and initial states. The estimate provided by such a tracker is simply the mean of the Gaussian density for target state.

Set based estimation provides an alternative philosophy for tracking. Rather than a point estimate, the estimate obtained using a set based tracker is a set of possible target states. This set is guaranteed to contain the true target state provided the system has been accurately modelled. Another advantage of set based tracking is that it only requires bounds on the process and measurement noises. It makes no assumptions on how these noises are distributed, except that they must satisfy the specified bounds. This can provide a more robust estimate of target state than Kalman filter based trackers in the particular case where noises are non-Gaussian.

The aim of a set based tracker is to maintain a guaranteed bound on the target state at all times. This means that the EKF approach of approximating the non-linear measurement equation by its Taylor series expansion may not be used as it does not maintain a guaranteed bound. The measurement conversions used in the CMKF do not apply to set based estimation, as a set based estimator requires a bound on the measurement error rather than a Gaussian distribution approximation. The principles behind the CMKF do apply to set based tracking, and in this paper, we propose a measurement conversion procedure specific to set based tracking. The premise of maintaining a guaranteed bound on target state continues throughout the paper.

In Section 2 the problem is formulated, including a brief description of set based estimation and discussion of ellipsoidal overbounding. A measurement conversion procedure specific to set based tracking is described in Section 3, and included in this is an improvement to the conversion for certain sets of parameters. Section 4 includes results of monte carlo simulations and discussion. Conclusions are drawn in Section 5.

2 Problem Formulation

2.1 System Equations

The state of a target is described by Cartesian position and velocity, $\mathbf{x}_k = [x_k, \dot{x}_k, y_k, \dot{y}_k]'$. We assume that the target obeys a nearly constant velocity model,

$$\mathbf{x}_{k+1} = \mathbf{F}_k \mathbf{x}_k + \mathbf{v}_k \tag{1}$$

where $\mathbf{F}_k = \begin{bmatrix} \mathbf{F} & \mathbf{0} \\ \mathbf{0} & \mathbf{F} \end{bmatrix}$ is the transition matrix and $\mathbf{v}_k$ is the process noise. Here $\mathbf{F} = \begin{bmatrix} 1 & T \\ 0 & 1 \end{bmatrix}$ where T is the time increment between updates. Rather than requiring statistical properties of the noise $\mathbf{v}_k$, the set based framework only requires that it be bounded, with the bound known,

$$\mathbf{v}_k \in \mathbf{\Omega}_Q(k). \tag{2}$$

The most simple assumption for the measurement equation is that the measurements are a linear function of the state parameters,

$$\mathbf{z}_k = \mathbf{H}_k \mathbf{x}_k + \mathbf{w}_k, \tag{3}$$

where $\mathbf{H}_k$ describes the relationship between state and measurement. The measurement noise is assumed bounded,

$$\mathbf{w}_k \in \mathbf{\Omega}_R(k). \tag{4}$$

Where measurements are of position only (as is common in target tracking), $\mathbf{H}_k$ is given by

$$\mathbf{H}_k = \begin{bmatrix} 1 & 0 & 0 & 0 \\ 0 & 0 & 1 & 0 \end{bmatrix}. \tag{5}$$

2.2 Set Based Estimation

The concept of set based estimation may be attributed to Schweppe [5, 6].

As described in the system equations above, both the process and measurement noise are assumed to belong to a bounded set, denoted $\mathbf{\Omega}_Q(k)$ and $\mathbf{\Omega}_R(k)$ respectively. This means that the noises may be correlated or biased, and may have any distribution provided its support matches the bound. The initial state is assumed to be drawn from some set, $\mathbf{\Omega}(0|0)$; this set may encompass the entire state space.

The optimal set based estimator involves two steps, a time update and an observation update. In the time update, the estimate from time $k-1$, $\mathbf{\Omega}(k-1|k-1)$, is projected forward to time k through the target trajectory model (ignoring the process noise) to give $\widetilde{\mathbf{\Omega}}(k|k-1)$. This set is not guaranteed to contain the target state at time k as it does not take into account the additive process noise. To obtain a guaranteed bound at time k, the set bounding the process noise, $\mathbf{\Omega}_Q(k-1)$, is vector summed to $\widetilde{\mathbf{\Omega}}(k|k-1)$. This accounts for any combination of true target state, $\mathbf{x}_k$ at time and process noise $\mathbf{v}_{k-1}$. Symbolically, the time update proceeds as

$$\mathbf{\Omega}(k|k-1) = \widetilde{\mathbf{\Omega}}(k|k-1) \oplus \mathbf{\Omega}_Q(k-1), \tag{6}$$

where $\oplus$ denotes a vector sum operation.

The observation update stage occurs after a measurement $\mathbf{z}_k$ is received at time k. The true target state is guaranteed to lie within the measurement noise bounds constructed about the measurement $\mathbf{z}_k$, this set is denoted $\mathbf{\Omega}_R^z(k)$. By its construction, the target state is also guaranteed to lie in the prediction set, $\mathbf{\Omega}(k|k-1)$. Thus, the true target state must lie in the intersection of these regions. The updated estimate, $\mathbf{\Omega}(k|k)$, is defined by

$$\mathbf{\Omega}(k|k) = \mathbf{\Omega}(k|k-1) \cap \mathbf{\Omega}_R^z(k). \tag{7}$$

This process is used iteratively to describe a guaranteed bound on the true target state over time.

In practice, this algorithm suffers from increasing complexity over time. A typical approach to counter this problem is to use ellipsoids to overbound the set of possible states in both the time and observation updates.

An ellipsoid may be completely described by its centre, $\mathbf{a}$, and matrix, $\mathbf{A}$,

$$\varepsilon(\mathbf{a}, \mathbf{A}) = \{\mathbf{x} : (\mathbf{x}-\mathbf{a})' \mathbf{A}^{-1} (\mathbf{x}-\mathbf{a}) \leq 1\}. \tag{8}$$

This notation for an ellipsoid will be used throughout the paper.

The process and measurement noises are assumed to be bounded by ellipsoids, as is the initial target state

$$\mathbf{v}_k \in \mathbf{\Omega}_Q(k) = \varepsilon(\mathbf{0}, \mathbf{Q}_k) \tag{9}$$

$$\mathbf{w}_k \in \mathbf{\Omega}_R(k) = \varepsilon(\mathbf{0}, \mathbf{R}_k) \tag{10}$$

$$\mathbf{x}_0 \in \mathbf{\Omega}(0|0) = \varepsilon(\mathbf{x}_{0|0}, \mathbf{P}_{0|0}) \tag{11}$$

Introducing the overbounding, the time update becomes

$$\mathbf{\Omega}(k|k-1) = \varepsilon(\mathbf{x}_{k|k-1}, \mathbf{P}_{k|k-1}) \supseteq \widetilde{\mathbf{\Omega}}(k|k-1) \oplus \mathbf{\Omega}_Q(k-1) \tag{12}$$

where, as before, $\widetilde{\mathbf{\Omega}}(k|k-1)$ is the projection of the estimate at time $k-1$ to time k. For the linear target trajectory model of equation (1), $\widetilde{\mathbf{\Omega}}(k|k-1)$ becomes

$$\widetilde{\mathbf{\Omega}}(k|k-1) = \varepsilon(\mathbf{F}_{k-1}\mathbf{x}_{k-1|k-1}, \mathbf{F}_{k-1}\mathbf{P}_{k-1|k-1}\mathbf{F}'_{k-1}). \tag{13}$$

The centre vector and matrix describing a parametric family of ellipsoids overbounding this vector sum [7, 8] have the form

$$\mathbf{x}_{k|k-1} = \mathbf{F}_{k-1}\mathbf{x}_{k-1|k-1} \tag{14}$$

$$\mathbf{P}_{k|k-1} = (p_k^{-1}+1)\mathbf{F}_{k-1}\mathbf{P}_{k-1|k-1}\mathbf{F}'_{k-1} + ... \\ (p_k+1)\mathbf{Q}_{k-1}, \tag{15}$$

where the parameter $p_k > 0$ may be used to minimise some aspect of the ellipsoid. We will use the minimum volume overbounding ellipsoid as derived by Chernous'ko [7] and described by Maksarov and Norton [8, 9].

A noisy measurement, $\mathbf{z}_k$, of target state is obtained at time k and may then be used to update the estimate according to

$$\mathbf{\Omega}(k|k) = \varepsilon(\mathbf{x}_{k|k}, \mathbf{P}_{k|k}) \supseteq \mathbf{\Omega}(k|k-1) \cap \mathbf{\Omega}_R^z(k) \tag{16}$$

where $\mathbf{\Omega}_R^z(k) = \varepsilon(\mathbf{z}_k, \mathbf{R}_k)$ is the measurement error ellipsoid constructed about the measurement. Following the derivation of Schweppe [5], also described in [8], a parametric family of ellipsoidal overbounds for the intersection of (16) have centre

$$\mathbf{x}_{k|k} = \mathbf{x}_{k|k-1} + \mathbf{L}_k \nu_k \tag{17}$$

where

$$\nu_k = \mathbf{z}_k - \mathbf{H}_k \mathbf{x}_{k|k-1} \tag{18}$$

is the innovation, and the gain term is given by

$$\mathbf{L}_k = \mathbf{P}_{k|k-1}\mathbf{H}'_k[\mathbf{H}_k\mathbf{P}_{k|k-1}\mathbf{H}'_k + q_k^{-1}\mathbf{R}_k]^{-1} \tag{19}$$

The matrix describing the shape of the ellipsoid is given by

$$\mathbf{P}_{k|k} = \beta_k(q_k)[(\mathbf{I}-\mathbf{L}_k\mathbf{H}_k)\mathbf{P}_{k|k-1}(\mathbf{I}-\mathbf{L}_k\mathbf{H}_k)' + q_k^{-1}\mathbf{L}_k\mathbf{R}_k\mathbf{L}'_k], \tag{20}$$

where the scalar function of the parameter is given by

$$\beta_k(q_k) = 1 + q_k - \nu_k'[q_k^{-1}\mathbf{R}_k + \mathbf{H}_k\mathbf{P}_{k|k-1}\mathbf{H}_k']^{-1}\nu_k. \quad (21)$$

The scalar parameter $q_k \geq 0$ may be selected to optimise some aspect of the intersection overbound. We will use the minimum volume overbound described by Maksarov and Norton [8, 9].

3 Range Bearing Measurement Conversion

3.1 Range-Bearing Measurements

Rather than the linear measurement equation (3), we are instead assuming that measurements of the target are range, r_k, and bearing, θ_k. These are given by non-linear functions of the target state parameters,

$$r_k = \sqrt{x_k^2 + y_k^2} + \gamma_k, \quad (22)$$

$$\theta_k = \tan^{-1}\left(\frac{x_k}{y_k}\right) + \delta_k \quad (23)$$

where bearing θ_k is taken in a clockwise direction from the y-axis. The measurement errors are bounded,

$$|\gamma_k| \leq \Delta r, \quad (24)$$

$$|\delta_k| \leq \Delta\theta. \quad (25)$$

This results in a range-bearing measurement error region given by

$$\begin{aligned}\mathbf{\Omega}_R^*(k) = \{(x,y) : (r_k - \Delta r \leq \sqrt{x^2+y^2} \leq r_k + \Delta r) \cap \\ (\theta_k - \Delta\theta \leq \tan^{-1}\left(\frac{x}{y}\right) \leq \theta_k + \Delta\theta)\}\end{aligned} \quad (26)$$

Constructing this region in Cartesian space results in a range-bearing measurement cell shaped like a sector of an annulus. The geometry is illustrated in Figure 1.

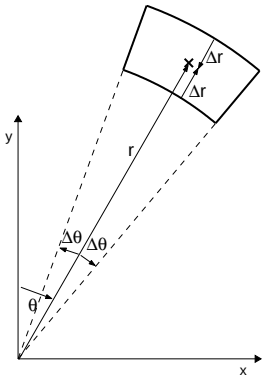

Fig. 1: Geometry of range-bearing measurement error cell

3.2 Range-Bearing Measurement Cell Overbound

In theory, the range-bearing error region, $\mathbf{\Omega}_R^*(k)$, may be incorporated directly into the optimal filter as the measurement error region. However, this is not feasible for practical purposes, where the implementation is the ellipsoidally overbounded algorithm described in Section 2.2. To incorporate the range bearing measurements into this algorithm, we are proposing a measurement conversion procedure where the range-bearing measurement cell is overbounded by an ellipse for use directly in the ellipsoidal version of the set based estimator.

Firstly note that, without loss of generality, the range bearing measurement error region may be assumed to be centred on the x-axis. This may be achieved simply by rotation so that the bearing measurement coincides with the x-axis. The error region is then symmetric about the x-axis.

This symmetry suggests that an overbounding ellipse should also have an axis along the x-axis. The centre of the ellipse must then be along the x-axis and the other axis of the ellipse must be parallel to the y-axis. The overbounding ellipse may thus be defined by the set

$$\mathbf{\Omega}_R = \{(x,y) : \frac{(x-a)^2}{u^2} + \frac{y^2}{v^2} \leq 1\}. \quad (27)$$

This is equivalent to the ellipsoid $\varepsilon(\mathbf{z}_k^x, \mathbf{R}_k^x)$, where

$$\mathbf{z}_k^x = \begin{bmatrix} a \\ 0 \end{bmatrix}, \quad (28)$$

$$\mathbf{R}_k^x = \begin{bmatrix} u^2 & 0 \\ 0 & v^2 \end{bmatrix}, \quad (29)$$

and the superscript x is used to denote the fact that the measurement cell has been rotated to lie on the x-axis. The rotation required to return the range-bearing error to its original orientation is described by the matrix,

$$\mathbf{\Gamma}_\theta = \begin{bmatrix} \sin(\theta) & -\cos(\theta) \\ \cos(\theta) & \sin(\theta) \end{bmatrix}, \quad (30)$$

noting that the bearing is taken as clockwise from the y-axis.

The converted measurement is then obtained by applying this rotation to give $\mathbf{\Omega}_R(k) = \varepsilon(\mathbf{z}_k, \mathbf{R}_k)$ where $\mathbf{z}_k = \mathbf{\Gamma}_\theta\mathbf{z}_k^x$ and $\mathbf{R}_k = \mathbf{\Gamma}_\theta\mathbf{R}_k^x\mathbf{\Gamma}_\theta'$.

3.2.1 Three Point Bound

The extreme points of the range-bearing cell are illustrated by asterisks in Figure 2(a). The points with minimum x-value are denoted B_1 and B_5 in the figure and are attained at $(r - \Delta r)[\cos(\Delta\theta), \pm\sin(\Delta\theta)]$. The maximum x-value is attained at $(r + \Delta r, 0)$ and is denoted B_3 in the figure. The minimum and maximum y-values are denoted B_4 and B_2 respectively and are given by $(r + \Delta r)[\cos(\Delta\theta), \pm\sin(\Delta\theta)]$.

Since the range-bearing measurement cell and its overbounding ellipse are symmetrical about the x-axis, if one of B_1 and B_5 or one of B_2 and B_4 are contained in the bound, the other will also be contained. This means that we only need to ensure that point B_1 given by $(r - \Delta r)[\cos(\Delta\theta), \sin(\Delta\theta)]$ is contained in the bound to ensure that B_5 is contained in the bound. Similarly, we only need to ensure that B_2 is contained in the bound to ensure that B_4 is contained in the bound.

Equation (27) defining the overbounding ellipse is described by 3 parameters, a, u, and v. It is possible to make

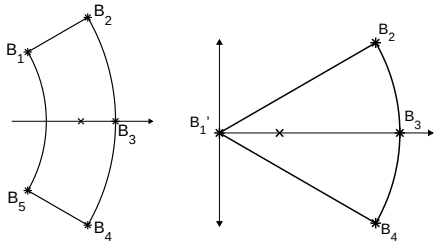

Fig. 2: Range Bearing measurement cell geometry when oriented along the x-axis (a) for $r > \Delta r$ and (b) for $r \leq \Delta r$. The extreme points of the regions are labelled.

the edge of the ellipse go through each of the five extreme points by solving the equality of Equation (27),

$$\frac{(x-a)^2}{u^2} + \frac{y^2}{v^2} = 1 \tag{31}$$

with (x, y) substituted for each of the three points, B_1, B_2 and B_3. That is, solving three simultaneous equations in three unknowns.

Substituting point B_3 into Eqn. (31) and rearranging gives u^2 as a function of a,

$$u^2 = (r + \Delta r - a)^2. \tag{32}$$

Substituting this, and point B_1 into Eqn. (31) gives v^2 as a function of a,

$$v^2 = \frac{(r-\Delta r-a)^2(r-\Delta r)^2\sin^2(\Delta\theta)}{(r+\Delta r-a)^2 - ((r-\Delta r)\cos(\Delta\theta)-a)^2}. \tag{33}$$

Finally, substituting (32), (33) and point B_2 into Eqn. (31) and rearranging gives

$$a = \frac{r(r+\Delta r)}{2r - (r-\Delta r)\cos(\Delta\theta)}. \tag{34}$$

The equations for u^2 and v^2 may also be simplified by substituting in the value of a. The overbounding ellipse resulting from solving these equations is illustrated in Figure 3(a) for the case $r > \Delta r$.

Now consider the special case where $r - \Delta r \leq 0$. In this case, we assume that ranges cannot be negative (the bearing cannot be out by 180^o), so the region becomes the sector of a circle of radius $(r+\Delta r)$ between angles $(\theta-\Delta\theta)$ and $(\theta+\Delta\theta)$ from the y-axis. Again we may assume without loss of generality that a rotation has been performed placing the bearing line along the x-axis. This is illustrated in Figure 2. The ellipse must now pass through B_2 and B_3 as before, but this time the point denoted B_1' with coordinates $(0, 0)$ replaces the critical point B_1 from above. By symmetry, the centre of the ellipse must be halfway between the two points on the x-axis, and the x-axis radius of the ellipse, u, must also be the same,

$$a = u = \frac{1}{2}(r + \Delta r). \tag{35}$$

Finally, it may easily be shown that

$$v^2 = \frac{(r+\Delta r)^2\sin^2(\Delta\theta)}{4\cos(\Delta\theta)(1-\cos(\Delta\theta))}. \tag{36}$$

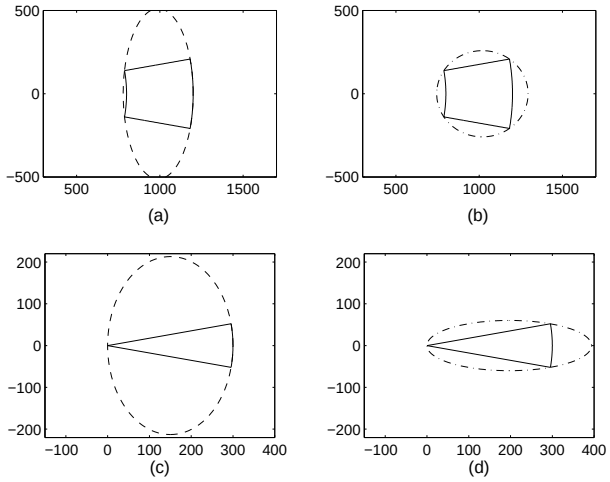

Fig. 3: Range-bearing measurement cell with overbounding ellipse for (a) $r > \Delta r$ and three point conversion, (b) $r > \Delta r$ and two point conversion, (c) $r \leq \Delta r$ and three point conversion and (d) $r \leq \Delta r$ and two point conversion

Again, the rotation back to the original bearing may be performed as described above to give the overbounding ellipse for the range-bearing measurement error region. An example of the overbounding ellipse generated using this procedure for the case $r \leq \Delta r$ is illustrated in Figure 3(c).

3.2.2 Two Point Minimum Volume Bound

For certain sets of values of r, Δr and $\Delta\theta$, the three point bound calculated above is not a particularly tight bound due to the fact that the edge of the ellipse is constrained to pass through all three extreme points. There are situations for small $\Delta\theta$ or large Δr, such as those illustrated in Figure 3, where a bound that is not constrained to pass through the point $(r + \Delta r, 0)$, but just to contain it, may achieve a smaller overall volume.

Consider the situation where the edge of the overbound must pass through points B_1 and B_2 from section 3.2.1. Substituting point B_1 into equation (31) results in an expression for v^2 as a function of u^2 and a,

$$v^2 = \frac{u^2(r-\Delta r)^2\sin^2(\Delta\theta)}{u^2 - ((r-\Delta r)\cos(\Delta\theta)-a)^2}. \tag{37}$$

Substituting this and the point B_2 into Eqn. (31) results in an expression for u^2 as a function of a,

$$u^2 = \frac{-a((r^2-(\Delta r)^2)\cos(\Delta\theta) - ar)}{r}. \tag{38}$$

Substituting this expression for u^2 into the expression for v^2 and simplifying gives v^2 as a function of a,

$$v^2 = \frac{-a((r^2-(\Delta r)^2)\cos(\Delta\theta) - ar)\sin^2(\Delta\theta)}{(a - r\cos(\Delta\theta))\cos(\Delta\theta)}. \tag{39}$$

The free parameter, a, defining the centre of the overbounding ellipse remains to be defined. Note that there cannot be an axis of symmetry through $x = r\cos(\Delta\theta)$ since this is exactly halfway between points B_1 and B_2 on the x-axis,

while the y-value of B_2 is strictly larger than that of B_1. The overbounding ellipse is symmetrical about $x = a$, and thus a must be strictly greater than $r\cos(\Delta\theta)$ for a bound to exist.

Since there are no more constraints on the overbounding ellipse (except that it contains B_3), a minimum area criterion may be used to define a. The area of the ellipse is proportional to the determinant of the matrix defining it. Define the function

$$\begin{aligned} A(a) &= |\mathbf{R}_k^x| && (40)\\ &= u^2 v^2 && (41)\\ &= \frac{a^2((r^2-(\Delta r)^2)\cos(\Delta\theta) - ar)^2\sin^2(\Delta\theta)}{r(a - r\cos(\Delta\theta))\cos(\Delta\theta)} && (42) \end{aligned}$$

By taking the derivative and equating this to zero, the only feasible value is given by $a = b\cos(\Delta\theta)$, where

$$b = \frac{5r^2 - (\Delta r)^2 + \sqrt{r^4 + 14r^2(\Delta r)^2 + (\Delta r)^4}}{6r}. \quad (43)$$

It is straightforward but tedious to show that this is a local minimum.

The maximum x-value of the overbounding ellipse may easily be shown to occur at $(a + u, 0)$. To ensure that point B_3 is contained in the ellipse, it must be the case that $r + \Delta r \leq a + u$. This occurs if $0 < \Delta\theta \leq \tilde{\theta}(r, \Delta r)$, where

$$\tilde{\theta}(r, \Delta r) = \cos^{-1}\left(\frac{\sqrt{r}(r + \Delta r)}{\sqrt{r}b + \sqrt{b(\Delta r)^2 + br - r^2}}\right). \quad (44)$$

When $\Delta\theta$ exceeds this bound, the three point bounding procedure described above is used. The two point overbounding procedure is used in Figure 3(b) for the case $r > \Delta r$, and it can easily be seen that the area is smaller than that attained by the three point bound.

Now consider the case where $r \leq \Delta r$. The two point minimum volume bound may also be derived for the special case of $r < \Delta r$ described earlier and depicted in Figure 2(b). The two critical points used here are the point B_2 used above and $(0, 0)$. Since the overbound is centred at $(a, 0)$ and must pass through the origin, the radius along the x-axis must match the centre, $u = a$. Following the same procedure as above, it may easily be shown that the value of a minimising the area of the overbound is given by

$$a = \frac{2}{3}(r + \Delta r)\cos(\Delta\theta). \quad (45)$$

The corresponding value of v^2 is given by

$$v^2 = \frac{4}{3}(r + \Delta r)^2\sin^2(\Delta\theta). \quad (46)$$

Again, the reverse rotation may be performed to obtain the overbound for the original orientation. Note that this minimum volume version applies only for

$$0 < \Delta\theta \leq \cos^{-1}(\frac{3}{4}) \simeq 41^o. \quad (47)$$

For larger bearing errors, the three point overbound described in Section 3.2.1 applies. An example of the overbound generated using this technique is shown in Figure 3(d) above, where it may be seen that the area attained by this bound is smaller than that using the three point bound.

It can be shown that the overbounding ellipse completely contains the range-bearing measurement error region for both the two and three point bounds and for all feasible values of r. Thus, the incorporation of these measurement conversions into a set based tracker satisfy the requirement of maintaining a guaranteed bound on the target state.

4 Results

In this section, the results of monte carlo simulations using both the three point and two point overbounds are presented.

We consider a target with nearly constant velocity motion as described in Section 2.1. The process noise is bounded by the ellipsoid $\varepsilon(\mathbf{0}, \mathbf{Q}_k)$ where

$$\mathbf{Q}_k = \begin{bmatrix} 100 & 0 & 0.25 & 0 \\ 0 & 2.56 & 0 & 0.0001 \\ 0.25 & 0 & 100 & 0 \\ 0 & 0.0001 & 0 & 2.56 \end{bmatrix}. \quad (48)$$

The initial target state is generated uniformly from the ellipsoid $\varepsilon(\mathbf{x}_0, \mathbf{P}_0)$, where $\mathbf{x}_0 = [5000, -10, 2000, -6]'$ and

$$\mathbf{P}_0 = \begin{bmatrix} 10000 & 0 & 400 & 0 \\ 0 & 9 & 0 & 0 \\ 400 & 0 & 10000 & 0 \\ 0 & 0 & 0 & 9 \end{bmatrix}. \quad (49)$$

Observations of the target are received at $T = 16$ second increments, and the tracker runs for 50 time intervals.

Measurements of the target are of range and bearing as described in equations (22) and (23) respectively. These range-bearing measurements are converted to an ellipsoid $\varepsilon(\mathbf{z}_k, \mathbf{R}_k)$ using the two and three point conversions described in Section 3.2. This allows the set based tracker to assume a linear measurement system as described in Equation (3), with $\mathbf{H}_k$ as described in (5). Note that this matrix may be used to project the ellipsoidal estimate into position space. Similarly, the matrix

$$\mathbf{H}_v = \begin{bmatrix} 0 & 1 & 0 & 0 \\ 0 & 0 & 0 & 1 \end{bmatrix} \quad (50)$$

may be used to project the ellipsoidal estimate into velocity space. These projections are used to calculate the volume of the projection of the estimate into position and velocity spaces in the first set of results. The volume of an ellipsoid is directly proportional to the determinant of the matrix describing it. The results of this section all use this determinant as a measure of the volume of the ellipsoids.

The first set of results used range error $\Delta r = 200m$, and bearing error $\Delta\theta = 2^o$. A set of 100 monte carlo runs were performed giving the results illustrated in Figure 4. In each of the graphs of the figure, the x-axis corresponds to the time step, k.

Figure 4(a) illustrates the average size of the determinant of the matrix defining the ellipsoidal estimate found by the set-based estimator using the two point conversion (dashed

line) and three point conversion (solid line). The two point conversion appears to perform much better than the three point conversion in this case.

Figure 4(b) illustrates the determinant of the projection of the ellipsoidal estimate into position space for the two point (dashed line) and three point (solid line) conversions. Also shown on these axes are the determinants of the matrices describing the two point (dotted line) and three point (dash-dotted line) measurement conversions. This illustrates the relative sizes of the overbound generated by the two point and three point measurement conversion, and it is quite clear that for the set of parameters used here, the two point conversion performs much better. This is the reason for the improved performance in the set based tracker using the two point measurement conversion over the three point conversion. Also of interest here are the changes in the size of the converted measurement ellipses with time. This is due to the change in range of the target with time - as the target approaches, the range decreases as does the range-bearing measurement cell. Somewhere between times 25 and 30, the target passes its closest point to the origin, and starts to move away again, increasing the size of the range-bearing measurement cell. This behaviour is reflected in both of the bounding ellipses for the range-bearing measurement cell.

This graph also illustrates an inherent problem in set based tracking with degenerate measurements. The projection of the estimate into measurement space is almost always larger than the measurement error as a result of the ellipsoidal overbounding performed at the time and observation updating steps. The only way this may potentially be avoided is if the noises, and in particular the measurement noise, reaches its bounds often, making the intersection between the prediction and measurement error region small.

Figure 4(c) shows the determinant of the projection of the estimate into velocity space for the set based tracker using the two point (dashed line) and three point (solid line) conversions, where it is again seen that the two point conversion results in a better bound on the target velocity. These graphs clearly show the benefit of using the two point minimum volume measurement conversion over the three point measurement conversion to reduce the size of the estimates at any step.

For Figure 5(a), the bearing error was fixed at 1^o and 5^o while the range error was incremented in steps of $50m$ from $50m$ to $1000m$. Similarly, for Figure 5(b), the range error was fixed at $100m$ and $500m$, while the bearing error was incremented in steps of 0.5^o between 0.5^o and 10^o. This allowed an investigation of the behaviour for different range-bearing error combinations. For each range-bearing error combination, the determinant of the matrix describing the set based tracker estimate was averaged over tracking steps 10-50, and over the 100 monte carlo runs performed.

As observed in the graphs of Figure 5, the three point bound does not change significantly as bearing error is changed over the values considered. This is because, especially where bearing error is small, the three point bound is a huge overbound on the measurement error region (as seen in Figure 3(a)), and does not change dramatically for small changes in bearing error. Both the two and three point bounds grow as the range error grows. For large bearing errors, the performance of the two point conversion approaches that of the three point conversion, due to the fact that the two point conversion is not feasible for large bearing errors and reverts to the three point conversion in that case anyway. However, as range error increases, the performance of the two point conversion improves increasingly over the three point conversion. The two point conversion performs best for small bearing errors, but is still in general an improvement over the three point conversion, particularly for large range errors. It is recommended that the two point overbounding procedure is used for measurement conversion for the set based tracker.

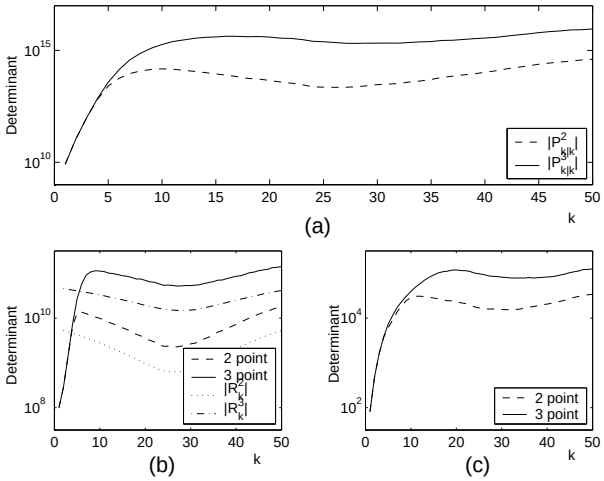

Fig. 4: Results of a monte carlo run with $\Delta r = 200m$ and $\Delta\theta = 2^o$ for two point (dashed) and three point (solid) measurement conversion; (a) $|\mathbf{P}_{k|k}|$ for each conversion, (b) $|\mathbf{H}_k\mathbf{P}_{k|k}\mathbf{H}_k'|$ for each conversion, and $|\mathbf{R}_{k|k}|$ for two point (dotted) and three point (dash-dotted) conversion, and (c) $|\mathbf{H}_v\mathbf{P}_{k|k}\mathbf{H}_v'|$ for each conversion.

5 Conclusion

Two procedures for converting range bearing measurements to Cartesian for a set based tracker have been presented in this paper. The first, referred to as three point measurement conversion, involves overbounding the measurement error region with an ellipse passing through all the critical points of the range-bearing measurement cell. A second procedure, referred to as two point conversion, is presented where the bound is only required to pass through two of the critical points, and contain the third. This uses a minimum volume criterion to optimise the bound, but is feasible only for bearing errors less than a critical bearing which is a function of the range and range error. Above this critical angle, the three point measurement conversion is used.

Monte carlo simulations have been performed using both conversions. These simulations demonstrate the benefit of using the two point conversion over the three point conversion, particularly for small bearing errors and/or for large range errors. It is recommended that the two point conversion be adopted to convert range-bearing measurements to

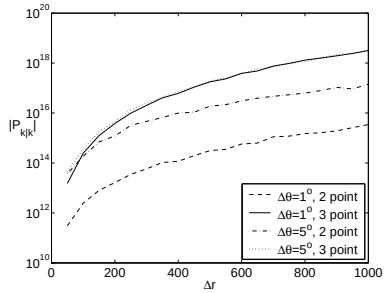

(a)

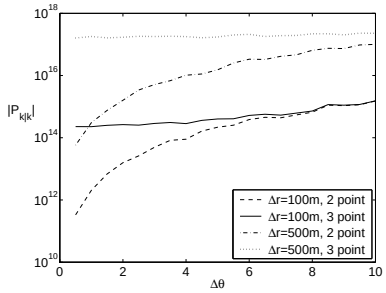

(b)

Fig. 5: Investigation of volume of set based tracker estimates with two and three point measurement conversions (a) for $\Delta\theta$ fixed at 1^o and 5^o and Δr varying from $50m$ to $1000m$ in steps of $50m$, and (b) for Δr fixed at $100m$ and $500m$ and $\Delta\theta$ varying from 0.5^o to 10^o in steps of 0.5^o.

a Cartesian bound for use in a set based tracker.

Acknowledgements

The authors would like to thank Prof. Rob Evans and Prof. Bill Moran for useful discussions relating to this work.

References

[1] Samuel S. Blackman and Richard Popoli. *Design and Analysis of Modern Tracking Systems*. Artech House, Boston, MA, USA, 1999.

[2] Y. Bar-Shalom and X-R. Li. *Multitarget-Multisensor Tracking: Principles and Techniques*. YBS, Storrs, CT, USA, 1995.

[3] D. Lerro and Y. Bar-Shalom. Tracking with debiased consistent converted measurements versus ekf. *IEEE Trans. Aero. Elec. Sys.*, 29(3):1015–1022, 1993.

[4] M. Longbin, S. Xiaoquan, Z. Yiyu, S. Z. Kang, and Y. Bar-Shalom. Unbiased converted measurements for tracking. *IEEE Trans. Aero. Elec. Sys.*, 34(3):1023–1027, 1998.

[5] F. C. Schweppe. Recursive state estimation: unknown but bounded errors and system inputs. *IEEE Trans. Auto. Control*, 13(1):22–29, 1968.

[6] F. C. Schweppe. *Uncertain Dynamic Systems*. Prentice-Hall Inc., Englewood Cliffs, NJ, USA, 1973.

[7] F. L. Chernous'ko. Optimal guaranteed estimates of indeterminacies with the aid of ellipsoids, i. *Engrg. Cybernetics*, 18(3):1–9, 1980.

[8] D. G. Maksarov and J. P. Norton. State bounding with ellipsoidal set description of the uncertainty. *Int. J. Control*, 65(5):847–866, 1996.

[9] D. G. Maksarov and J. P. Norton. Computationally efficient algorithms for state estimation with ellipsoidal approximations. *Int. J. Adapt. Control Signal Process.*, 16(6):411–434, 2002.